The correlation of blue shift of photoluminescence and morphology of silicon nanoporous

Batool E. B. Al-Jumaili, Zainal A. Talib, Josephine L. Y., Suriati B. Paiman, Naser M. Ahmed, Abdulmajeed H. J. Al-Jumaily, Asmiet Ramizy, Sinan A. Abdulateef, Ibrahim B. Muh'd, and Manahil E. E. Mofdal

Citation: AIP Conference Proceedings **1733**, 020019 (2016); doi: 10.1063/1.4948837
View online: http://dx.doi.org/10.1063/1.4948837
View Table of Contents: http://scitation.aip.org/content/aip/proceeding/aipcp/1733?ver=pdfcov
Published by the AIP Publishing

The Correlation Of blue Shift of Photoluminescence and Morphology of Silicon Nanoporous

Batool E. B. Al-Jumaili [1,4,a], Zainal A. Talib[1], Josephine L. Y[1], Suriati B. Paiman[1] , Naser M. Ahmed[3], Abdulmajeed H.J. Al-Jumaily[2] , Asmiet Ramizy[4] ,Sinan A. Abdulateef[3], Ibrahim B. Muh'd[1], & Manahil E. E. Mofdal[1]

[1]Department of Physics, (UPM), Serdang, Selangor 43400, Malaysia
[2]Department of Computer and Communication Systems Engineering, Universiti Putra Malaysia (UPM), Serdang, Selangor 43400, Malaysia
[3] School of Physics, USM, 11800 Penang, Malaysia
[4] Department of Physics, Anbar University
[a] batooleneaze@gmail.com

Abstract. Porous silicon with diameters ranging from 6.41 to 7.12 nm were synthesized via electrochemical etching by varied anodization current density in ethanoic solutions containing aqueous hydrofluoric acid up to 65mA/cm^2.The luminescence properties of the nanoporous at room temperature were analyzed via photoluminescence spectroscopy. Photoluminescence PL spectra exhibit a broad emission band in the range of 360-700 nm photon energy. The PL spectrum has a blue shift in varied anodization current density; the blue shift incremented as the existing of anodization although the intensity decreased. The current blue shift is owning to alteration of silicon nanocrystal structure at the superficies. The superficial morphology of the PS layers consists of unified and orderly distribution of nanocrystalline Si structures, have high porosity around (93.75%) and high thickness 39.52 μm.

Keywords: Porous silicon, Electrochemical etching, Photoluminescence, porosity, Diameters.

INTRODUCTION

Porous silicon was attracted the consideration of several empirical and theoretical investigation[1,2], owing to its distinct photoluminescence within the visible range of the electromagnetic spectrum at room temperature[3]. Porous silicon enters the application in a wide number of fields such as microelectronics, optoelectronics[4], chemical [5] and biological [6] sensors and biomedical devices[7]. Nevertheless, the instability of the Si–Hx, that could undergo automatically to oxidation from ambient atmosphere which leads to deterioration of the layers structure and photoluminescence features, still the essential issue of commercial applications of PS[8]. In the current report, investigate the Photoluminescence (PL) properties of porous silicon films as a function of etching current flux. Porous silicon organized by Photo-electrochemical etching this way is catchy in the formation of porous n-type Si reason of the facility with which porous films could fabricated overhead a wide area of the specimens and the regularity of those films [9]. In this study, the optical characteristics and morphology of PS substrates were investigated. The outcomes demonstrate that the anodization current density is a significant factor that controls the etching ratio and morphology of the porous specimen. Therefore, this factor can be utilized to improve the optical features of electrochemical etched PS layers.

International Conference on Nano-electronic Technology Devices and Materials 2015 (IC-NET 2015)
AIP Conf. Proc. 1733, 020019-1–020019-5; doi: 10.1063/1.4948837
Published by AIP Publishing. 978-0-7354-1384-9/$30.00

EXPERIMENTAL

The porous structure were grown on slightly doped n-type Si (100) wafer via using a photo- electrochemical etching method. Earlier to the etching procedure, substrates were cleaned by sonication (15 min) in acetone, ethanol and diluted HF acid (10 wt. %) respectively to remove the oxide layer and dry them with nitrogen blow. The electrochemical etching procedure was conducted in a Teflon cell. The Si sample as an anode and Pt mesh was used as the counter electrode were linked to the external direct current (DC) power supply. The electrolyte consisted of admixture of 48% HF and ethanol 99.90% taken the mole rate of 1:4. Owing to the frenzied characteristic of the clean Si wafer, ethanol had been inserted into the aqueous HF solution to increment the wettability of the Si surface. Moreover, insertion ethanol well aid to eliminate the H bubbles which generated on the Si interface and as a consequence enhance the homogeneity of the PS layer [10,11]. The experiment was conducted at a steady etching duration 15 min for various anodization current density J of 15, 45 and 65 mA/cm2. The front side of silicon was irradiated by a halogen lamp (300 W) through the method of etching. It was recounted the holes are required to facilitate the dissolution reactions [10]. Wherefore, a halogen lamp was used to get a great concentration of holes for the etching procedure to occur. PSi samples were immersed in ethanol and dried underneath the nitrogen shower after the etching procedure. The visual view of porous specimen can see in **FIGUER1**.

The PL measurement was recorded at room temperature employ a Perkin Elmer, model: LS55 spectrometer. The superficial morphological alterations through anodization were spotted through an area of emission scanning electron microscopy FSEM (Nova NanoSEM 30series).

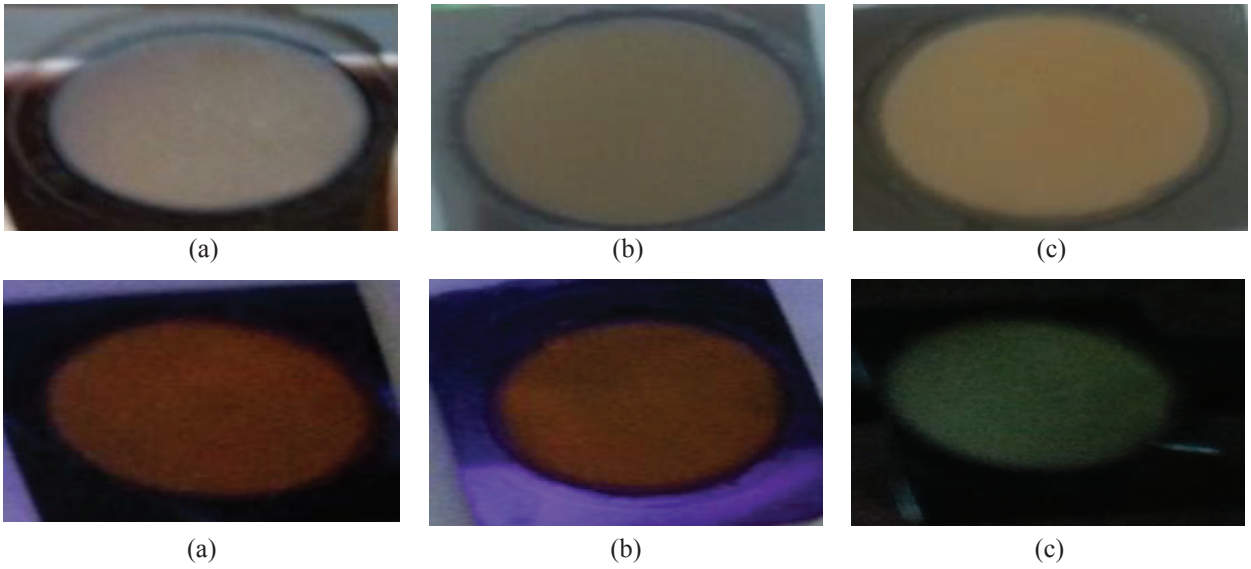

FIGURE 1. The PS surface after etching under room light (upper part) and UV excitation (lower part) formed at (a) 15 mA/cm^2, (b) 45 mA/cm^2,and (c) 65 mA/cm^2.

RESULTS AND DISCUSSION

The ratios of porosity and thickness were calculated via a gravimetric measurement [12,13]. The corresponding ratios for the PS that were etched below 15, 45, and 65 mA/cm^2 anodization current, were 40%, 86.66%, and 93.75% respectively and thickness ratios were 12.35 μm, 37.05 μm, 39,52 μm respectively. The total porosity and thickness of PS was obviously improved by raising the current density.

FIGUER2 shows the field emission scanning electron microscopy (FESEM) images of porous samples. The FESEM micrographs confirm that the current density has a considerable influence on the shape and size of the pores. The etched surfaces of the specimens (a) and (b) suffer from a shortage of regularity in the form of

heterogeneous pores. The moment that pits have formed, etching outcome anisotropic as the electrolyte hinder the passivation layer formation on the flat etching area stronger than on the perpendicular sidewalls [14]. Meanwhile extra etching, the initial vertical pores quickly become deeper, but also wider that obtained at (a), the holes are not clearly formed. The superficies of the Si contain separate pores amidst short tunnels and smooth walls. As the etching continues, the pores intersect progressively become more connected to each other at (b) which resulted the edges of the remaining non-etched layer to be observable. That may be due to the insufficient etching time to dissolve all the chemically treated area. Nevertheless, the FE-SEM image of specimen (c) exposes a higher porosity with a regular porous surface. The high current influx into the fabrication of the sample (c) raised the density of its pores, thereby participation in the high porosity of this specimen.

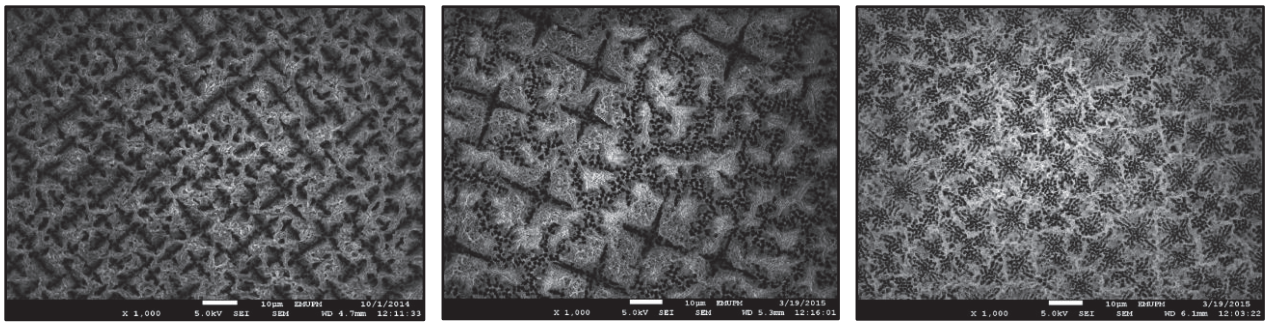

(a) (b) (c)

FIGURE 2. FESEM images of the PS formed at (a) 15 mA/cm^2, (b) 45 mA/cm^2, and (c) 65 mA/cm^2.

The luminescence spectrum of the PSi specimens etched in various current densities are depicted in **FIGURE 3.** The vastly accepted opinion for luminescence spectrum is the establishment of the quantum confinement principle. It is explained that emissions arise from the electron–hole recombination in the quantum wells within separated energy levels. Those energy levels were created via bulk areas which are discrete through nanocrystal particles [15, 9]. The Photoluminescence spectrum of the PSi specimens was highly shifted to short wavelength in comparison with PL of bulk Si. The greatest Photoluminescence shift in the PSi specimen C compatible with the quantum confinement principle. Meanwhile, the porosity was incremented, the mean size of silicon nanocrystal structure reduced and the shifted to short wavelength is occurring to the Photoluminescence spectrum. The measure of the size of the PS nanostructure required to create orange, yellow and green PL can be acquired from the effective mass theory. Supposing infinite potential barriers, the energy gap E for 3D confined Si should diverse such [16].

$$E=E_g+\frac{h^2}{2d^2}\left(\frac{1}{m_e^*}+\frac{1}{m_h^*}\right) \quad (1)$$

Where Eg=1.12 eV is the band gap of the bulk Si, d is the diameter of the particle and m_e^*=0.26m_0 is effective mass of the electron and m_h^*=0.69m_0 is the hole effective mass at 300 K. Consequently, it can estimated those the detected PL peaks at 590, 561 and 532 nm are caused by the Si nanocrystal, results are outlined in Table (1).

Table 1. PL peak, band gap and intensity values observed of different current densities 15, 45, 65 mA/cm².

Current Density (mA/cm2)	Wavelength peak (nm)	Energy gap of PSi (nm)	Diameter of Psi (nm)
15	590	2.10	7.1
45	561	2.21	6.7
65	532	2.33	6.4

The photoluminescence intensities are influenced by the employment of anodization current flux. It is related with the growing surface rough, in addition, the huge surface area of the PSi structures [17]. Consequently, the intensity of photoluminescence showed a decreasing trend with an increasing in current density and attributed this decline in the PL intensity is generally to a large number of dangling bonds in PSi versus to that in the bulk Si, a large number of dangling bonds in the PS exists due to a formidable opening area of the surface in the air. These bonds can supply a significant channel for non-radiative recombination [18,19]. At the same time, size dispersion is too an essential factor, due to the actuality that while the size distribution becomes broader, the PL intensity will become lower[20]. Meier et al. [21] studied the impact of sizes distribution on the performance of optical emission and find that for nanoporous silicon, the size distribution is an essential factor in determine the PL.

This is exhibited in the current density of 65 mA/cm², where the energy gab is reached to a higher value of 2.33 eV. Such a result was found to be similar in [18].

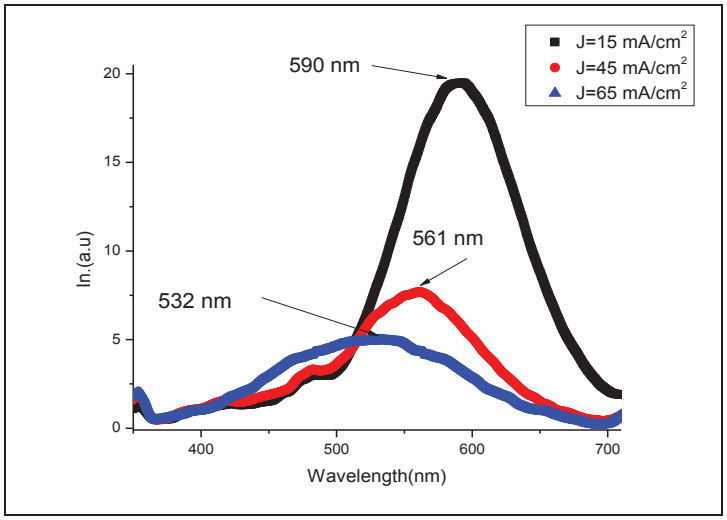

FIGURE 3. Room temperature photoluminescence spectra of PS samples prepared at different current density 15, 45 and 65 mA/cm².

CONCLUSIONS

The porous Si at different anodization current densities was successfully fabricated by electrochemical etching. The outcomes exhibited that the density of anodization current was a significant factor which governs the pores density of the porous specimen. The superficial morphology of the PS exhibited fine structure and non-cracked formation. The impact of diverse the anodization current on the morphology of PS surface was noticed. When the anodization current incremented to 65 mA/cm^2, the development of pore structures is varied in shape besides size. The pores structures were confined to little sizes. This issue is well confirmed by the measurement

photoluminescence analysis. The high-quality specimen exhibited peak of photoluminescence for almost high blue shift that proof a vast regularity in this layer also porosity owing to a reduction in a Si crystallinity size while utilized the big density of anodization current.

ACKNOWLEDGEMENTS

This work was supported by the Ministry of Higher Education Malaysia under Exploratory Research Grant Scheme Grant and the Ministry of Higher Education Iraq Grant.

REFERENCES:

1. J. Lugo, Sol. Energy Mater. Sol. Cells **52**, 239–249 (1998).
2. O. Bisi, S. Ossicini, and L. Pavesi, Surf. Sci. Rep. **38**, 1–126 (2000).
3. A. E. Pap, K. Kordás, J. Vähäkangas, A. Uusimäki, S. Leppävuori, L. Pilon, and S. Szatmári, Opt. Mater. (Amst) **28**, 506–513 (2006).
4. S. Chen, Y. Huang, and B. Cai, Solid. State. Electron. **49**, 940–944 (2005).
5. L. T. Canham, Appl. Phys. Lett. **57**, 1046 (1990).
6. S. Lazarouk, P. Jaguiro, S. Katsouba, G. Masini, S. La Monica, G. Maiello, and A. Ferrari, Appl. Phys. Lett., **68**, 2108 (1996).
7. P. Steiner and W. Lang, Thin Solid Films **255**, 52–58 (1995).
8. A. Richter, P. Steiner, F. Kozlowski, and W. Lang, IEEE Electron Device Lett. **12**, 691–692 (1991).
9. N. Naderi and M. R. Hashim, Mater. Res. Bull. **48**, 2406–2408(2013).
10. N. I. Rusli, M. Tanikawa, M. R. Mahmood, K. Yasui, and A. M. Hashim, Materials (Basel). **5**, 2817–2832 (2012).
11. H. R. Abd, Y. Al-Douri, N. M. Ahmed, and U. Hashim, Int. J. Electrochem. Sci. **8**, 11461–11473(2013).
12. K. a. Salman, K. Omar, and Z. Hassan, Sup.lat. Microstruct. **50**, 517–528(2011).
13. Y. Wu, M. Hu, Y. Qin, X. Wei, S. Ma, and D. Yan, Sensors Actuators, B Chem. **195**, 181–188 (2014).
14. M. Steglich, T. Käsebier, M. Zilk, T. Pertsch, E.-B. Kley, and A. Tünnermann, J. Appl. Phys. **116**, 173503 (2014).
15. A. Ramizy, W. J. Aziz, Z. Hassan, K. Omar, and K. Ibrahim, Opt. - Int. J. Light Electron Opt. **122**, 2075–2077 (2011).
16. A. F. Abd Rahim, M. R. Hashim, and N. K. Ali, Phys. B Condens. Matter. **406**, 1034–1037 (2011).
17. N. Naderi, M. R. Hashim, and T. S. T. Amran. Sup.lat. Microstruct **51**, 626–634 (2012).
18. A. M. Alwan and M. S. M. Jawad, Eng. Tech. J. **31**, 291–299(2013).
19. W. Henley, Y. Koshka, J. Lagowski, and J. Siejka, J. Appl. Phys. **87**, 7848 (2000).
20. P. F. Trwoga, A. J. Kenyon, and C. W. Pitt, J. Appl. Phys. **83**, 3789 (1998).
21. C. Meier, A. Gondorf, S. Lüttjohann, A. Lorke, and H. Wiggers, J. Appl. Phys. **101**, 103112 (2007).